Lab on a Chip

Nanofluidic analytical system integrated with nanochannel open/close valves for enzyme-linked immunosorbent assay

Journal:	*Lab on a Chip*
Manuscript ID	LC-ART-09-2022-000881.R1
Article Type:	Paper
Date Submitted by the Author:	26-Nov-2022
Complete List of Authors:	Sano, Hiroki; The University of Tokyo, Kazoe, Yutaka; Keio University Faculty of Science and Technology Graduate School of Science and Technology, System Design Enigineering; The University of Tokyo, Ohta, Ryoichi; The University of Tokyo, Shimizu, Hisashi; The University of Tokyo, Collaborative Research Organization for Micro and Nano Multifunctional Devices Morikawa, Kyojiro; The University of Tokyo, School of Engineering Kitamori, Takehiko; The University of Tokyo,

Nanofluidic analytical system integrated with nanochannel open/close valves for enzyme-linked immunosorbent assay

Hiroki Sano,[a] Yutaka Kazoe,*[b] Ryoichi Ohta,[d] Hisashi Shimizu,[d] Kyojiro Morikawa,[c,d] and Takehiko Kitamori*[c,d,e]

[a] Department of Applied Chemistry, School of Engineering, The University of Tokyo, 7-3-1 Hongo, Bunkyo, Tokyo 113-8656, Japan

[b] Department of System Design Engineering, Faculty of Science and Technology, Keio University, 3-14-1 Hiyoshi, Kohoku, Yokohama, Kanagawa 223-8522, Japan

[c] Institute of Nanoengineering and Microsystems, Department of Power Mechanical Engineering, National Tsing Hua University, No. 101, Section 2, Kuang-Fu Road, Hsinchu 300044, Taiwan

[d] Collaborative Research Organization for Micro and Nano Multifunctional Devices, The University of Tokyo, 7-3-1 Hongo, Bunkyo, Tokyo 113-8656, Japan

[e] Department of Biomedical Engineering, Faculty of Engineering, Lund University, 221 00 Lund, Sweden

*Correspondence

Dr. Yutaka Kazoe, Department of System Design Engineering, Faculty of Science and Technology, Keio University, 3-14-1 Hiyoshi, Kohoku, Yokohama, Kanagawa 223-8522, Japan

Email: kazoe@sd.keio.ac.jp

Phone: +81-45-566-1843

Fax: +81-45-566-1720

Dr. Takehiko Kitamori, Collaborative Research Organization for Micro and Nano Multifunctional Devices, The University of Tokyo, 7-3-1 Hongo, Bunkyo, Tokyo 113-8656, Japan

Email: kitamori@icl.t.u-tokyo.ac.jp

Phone: +81-3-5841-7231

Fax: +81-3-5841-6039

Abstract

There have been significant advances in the field of nanofluidics, and novel technologies such as single-cell analysis have been demonstrated. Despite the evident advantages of nanofluidics, fluid control in nanochannels for complicated analyses is extremely difficult because the fluids are currently manipulated by maintaining the balance of driving pressure. To address this issue, the use of valves will be essential. Our group previously developed a nanochannel open/close valve utilizing glass deformation, but this has not yet been integrated into nanofluidic devices for analytical applications. In the present study, a nanofluidic analytical system integrated with multiple nanochannel open/close valves was developed. This system consists of eight pneumatic pumps, seven nanochannel open/close valves combined with piezoelectric actuators, and an ultra-high sensitivity detector for non-fluorescent molecules. For simultaneous actuation of multiple valves, a device holder was designed that prevented deformation of the entire device caused by operating the valves. A system was subsequently devised to align each valve and actuator with a precision of better than 20 μm to permit the operation of valves. The developed analytical system was verified by analyzing IL-6 molecules using enzyme-linked immunosorbent assay. Fluid operations such as sample injection, pL-level aliquot sampling and flow switching were accomplished in this device simply by opening/closing specific valves, and a sample consisting of approximately 1,500 IL-6 molecules was successfully detected. This study is expected to significantly improve the usability of nanofluidic analytical devices and lead to the realization of sophisticated analytical techniques such as single-cell proteomics.

1. Introduction

Microfluidics has significantly advanced over the years and has been integrated with chemical operations such as mixing,[1] reaction systems,[2] and separation[3,4] to provide rapid and highly sensitive analyses.[5–7] Valves play an essential role in these sophisticated devices to allow accurate control of fluid flows. Among the numerous types of valves that have been reported over the past several decades (including diaphragm,[8–10] phase-changing,[11,12] ball,[13,14] and Laplace valves[15,16]), pneumatic inline channel open/close valves are currently the most widely used.[17–19] Because these units are constructed of soft materials such as polydimethylsiloxane, analyses are generally carried out using aqueous reagents. The ease of fabrication of these devices and their ease of integration at high densities has allowed their applications in laboratories and commercial products.[20,21]

Our group previously developed a method for the nano-fabrication of glass substrates.[22] This process allows the construction of ultra-small nanochannels with volumes on the femtoliter to picoliter size scale that enable the handling of single/countable molecules. On this basis, nano-unit operations (NUOs) were realized, including those in single molecule enzyme-linked immunosorbent assay (ELISA),[23] a picoliter-scale enzyme reactor,[24] and nanofluidic chromatography,[25] corresponding to chemical operations of molecule capture, enzymatic reaction and separation, respectively. The integration of these NUOs is expected to allow novel processes such as single-cell analysis. As an example, 13 unit operations were previously integrated on a nanofluidic device, leading to the quantification of interleukin (IL)-6 molecules secreted from a single B cell.[26]

However, fluid operations in current nanofluidic devices are conducted by adjusting the driving pressure of the reagents to maintain a pressure balance and control the direction of the flow inside nanochannels, which is extremely difficult. As such, the use of nanofluidic devices currently requires highly complex operations and so must be performed by skilled technicians. In addition, the number of chemical operations that can be controlled in one device is limited due to these challenges. In order to

achieve a higher level of integration and usability, the incorporation of valves in nanofluidic devices is essential. For this reason, our group previously developed a nanochannel open/close valve utilizing glass deformation.[27,28] Although the operation of a single valve was verified, integration of multiple valves and fluid operations for nanofluidic analyses using such valves has not yet been achieved.

The present study developed a nanofluidic analytical system comprising a nanofluidic device integrated with multiple valves, external pressure pumps and an ultrasensitive detector for non-fluorescent molecules. A system for controlling multiple valves comprising piezo-electric actuators and a device holder to prevent the entire deformation of device was constructed. In addition, a method for aligning the actuators and the valves was established. Based on the developed system, fluid control in nanochannels utilizing multiple valves was verified. Finally, the analytical system was demonstrated for cytokine analysis by ELISA utilizing nanofluidics.

2. Design of the system

The present nanofluidic analytical system consists of a nanofluidic device integrated with multiple valves, pneumatic pumps, piezoelectric actuators to operate the valves, piezo controllers, and a detector, as shown in Fig. 1. A holder is used to clamp the edges of the device and polytetrafluoroethylene screws are used to affix this holder as a connection between capillary tubes and the inlets of micro-/nanochannels to allow reagents to be flowed in. The nanochannel open/close valves are operated by applying a pressure of 3.2 GPa (that is, a force of 1 N on a circular area with a diameter of 75 μm) to a deformation area.[27,28] Piezoelectric actuators were selected for this purpose in conjunction with stainless steel pressing pins capable of applying sufficient force to the small circular areas. Each piezoelectric unit has dimensions of 1.1 mm × 0.8 mm × 10 mm and is fabricated by TOKIN Corp., Japan. The pressing pin has a diameter of 2 mm and a rectangular hole to allow insertion of the piezoelectric element. Holes, each 2 mm in diameter, are machined into the chip holder to allow the actuators to be directly set into the holder. The valves are

set 3.5 mm apart, representing the shortest distance possible based on the restrictions imposed by the machining process. The height at which the actuators are positioned is fixed by tightening a screw. The highly sensitive detection of countable molecules in the nanochannel is accomplished by using a differential interference contrast thermal lens microscope (DIC-TLM) as the detector.[29] Specifically, the DIC-TLM is employed to monitor changes in the refractive index of the solution based on the phase contrast resulting from nonradiative relaxation after light absorption by the analyte. This technique enables the detection of non-fluorescent molecules. Because the DIC-TLM incorporates a centimeter-sized objective lens and is placed both at the top and bottom of the device, the device holder must provide sufficient space above and below a specific area of the unit.

As a consequence of this unsupported space, this entire device could deform in the case that a load was applied to the valves. Moreover, when operating multiple valves, the opening/closing state of some valves would be affected by the application of force to others. To mitigate these issues, a device holder was designed having a component that supported the apparatus and reduced deformation of the entire device when operating the valves to less than approximately 1 nm, which is sufficiently smaller than the depth of the valve: 100 nm. The appropriate size of the support that reduced deformation of the device without interfering with the detectors was determined by numerical simulations based on the finite element method, using the COMSOL Multiphysics® 5.6 software package.[30] In these calculations, it was assumed that there would be no displacement of the edges clamped by the chip holder, and the size of the deformable area was set to 34 mm × 51 mm based on the position of the edges of the chip holder (Fig. 2). The distribution of the deformation across the pressing area is shown in Fig. 2. As indicated in Fig. 2(a), the maximum deformation was 1.2 μm when a load of 1 N was applied to a single valve in the center of the device. In the case that a force of 1 N was applied to a valve next to the first valve, the device was further deformed by more than 1 μm. Because this value exceeded the depth of the valve (100 nm), closing the second valve would open the first valve (which was initially closed), suggesting that independent

control of the valves would be impossible. Figure 2(b) shows the jig with a support under the valve area having a width, depth, and thickness of 7, 34, and 2 mm, respectively. The installation of the support in this manner reduced the maximum deformation of the entire device to 100 nm. In addition, with the support in place, actuation of the second valve resulted in an additional deformation of less than 1 nm, which was sufficiently small compared with the valve depth. Thus, this specially designed support for the chip holder prevented the effect of deformation caused by open/close operations of the valves and enable the independent control of multiple valves.

3. Experimental

3.1. Construction of analytical system

Based on the design described in Section 2, the analytical system shown in Fig. 3(a) was fabricated. In this system, the reagents were flowed into the channels using pneumatic pumps (ARGOS, Institution of Microchemical Technology, Kanagawa, Japan). The flow inside the channels and the operation of the valves were confirmed by observations using a fluorescence microscope (IX73, Olympus Corp., Tokyo, Japan), and the entire device could be moved to the stage of a DIC-TLM placed next to the fluorescence microscope and serving as a detector. As outlined in Section 2, the jig had a defined space open on the top and the bottom of the unit so that the objective lens of the detector could be integrated (Fig. 3(b)). In addition, a component to support the device was installed just below the valve-pressing area to prevent deformation without interfering with the detector (Fig. 3(c)). On the device substrate, multiple deformable parts were fabricated to serve as valves, each with a small area (1.5 mm in diameter) and a glass thickness of 30 μm. Valve chambers having a four-stepped structure were designed and installed below these deformable regions. The four steps in this structure were formed such that each valve chamber had a shape similar to that of the glass when undergoing deflection in response to a 1 N load applied to the deformable part in order to close the valve.[27,28]

3.2. Operation of multiple valves

In order to open/close the valves as designed, the actuators would ideally be aligned with the center of the valves. However, there will naturally be a positioning error between the actuator and the valve positions when the device is placed on the jig and manually fixed in place. The tolerable positioning error between the actuators and the valves was evaluated experimentally and determined to be 20 μm (see Fig. S1 for details), and so the alignment between the actuators and the valves was required to be within this level of precision.

Because the positioning of the actuators could not be independently controlled, the position of each valve had to coincide with the center of the corresponding jig hole. However, because the holes on the chip holder were mechanically fabricated, a positioning error on the order of 100 μm was unavoidable. To address this issue, the actual coordinates of the holes on the device holder were obtained, after which the required positioning of the valve chambers was determined (details are available in the Supplementary Information to this paper). Since the valve chambers were manufactured using a top-down nanofabrication method (described in Section 3.3), it was possible to produce each valve chamber at the same position as the corresponding hole on the device holder within an error on the micrometer level.

Even though the valves and the holes on the jig through which the actuators were inserted were designed to be at the same positions, the actual positioning of the valves and the actuators would not coincide perfectly because of an inevitable positioning error caused by manual setting process of the device into the device holder. For this reason, an alignment stage that enabled the positions of the actuators to be adjusted, such that each could be set above each valve within a positioning error of 20 μm, had to be developed. Using this newly developed system to align the actuators, the independent operation of the multiple valves was verified. After verifying operation of multiple valves, the operation repeatability was verified by performing flow switching using multiple valves.

3.3. Device for system verification

The operation of the newly developed system was verified by a demonstration of ELISA. The design of the device used for the verification trials is presented in Fig. 4. Based on a method of integrating NUOs,[31] the ELISA process was broken down into eight unit operations and converted into corresponding NUOs. The NUOs were connected using a total of seven valves: one valve for partitioning the sampling region and the analysis region, two valves for determining the volume of the sample, and four valves for flow switching to inject the reagents or washing buffer. The capture antibody was immobilized on the surface of the nanochannel in the analysis region (hereinafter referred to as the ELISA channel), and the surfaces of the nanochannels were modified with polyethylene glycol (PEG) to prevent non-specific adsorption of protein molecules.[23]

The microchannels, nanochannels and valve chambers were produced using a top-down nanofabrication method.[32] A fused silica substrate with a thickness of 0.7 mm (VIOSIL, Shin-Etsu Quartz Co., Ltd., Tokyo, Japan) was used for the lower substrate. Nanochannels were initially fabricated by electron beam (EB) lithography (ELS-7800K, Elionix Inc., Tokyo, Japan) followed by plasma etching (NLD-570, ULVAC Co., Ltd., Kanagawa, Japan). After this, valve chambers were fabricated between the nanochannels using a previously reported technique also based on EB lithography and plasma etching. Finally, microchannels were fabricated on the same substrate by photolithography followed by plasma etching. A substrate with a thickness of 0.3 mm (VIOSIL, Shin-Etsu Quartz Co., Ltd., Tokyo, Japan) was used as the upper substrate, and a wet etching process employing hydrofluoric acid was used to fabricate deformation parts with a thickness of 0.03 mm. For the purpose of the ELISA demonstration, aminopropyltriethoxysilane (APTES) was partially modified in the ELISA channel in order to immobilize the capture antibody.[23] The two substrates were subsequently washed in a manner that did not affect the modifications described above and then bonded together.[33] After bonding, the nanochannels were filled with ethanol for the following PEG modification, which prevents the non-specific adsorption of protein

molecules. Trimethoxysilane-PEG (MW=5,000) was dissolved in water/ethanol (5/95) solution at the concentration of 0.1 wt%. First, the microchannels and the nanochannels were filled with ethanol and then replaced to PEG solution. During this process the PEG silane molecules react with the silanol groups on the surface of the nanochannels and modify the channel surface. After 90 minutes of modification, the microchannels and the nanochannels were washed with ethanol for 15 minutes. Finally, bovine serum albumin (BSA) was pumped into the ELISA channel to block the adhesion sites and further prevent non-specific adhesion.[33]

3.4. Demonstration of ELISA

A demonstration of ELISA was carried out using a procedure previously reported by our group with a slight modification.[26] MAB206-500 anti-IL-6 antibody (clone 6708, R&D Systems, Inc., Minneapolis, MN, USA) was selected as the capture antibody in the ELISA channel. The washing buffer comprised 100 mM xylene-cyanol, 2 wt% BSA, 0.05% Tween 20, and 10 mM phosphate buffered saline (PBS). Xylene-cyanol is a colored molecule and was used to calibrate the detection system. The horseradish peroxidase (HRP)-conjugated antibody solution contained 1.5 μg/mL (10 nM) HRP-conjugated anti-IL-6 polyclonal antibody (Abcam, Cambridge, UK) in a buffer consisting of 2% BSA, 0.05% Tween 20, and 10 mM PBS. A 1.7 mM solution of 3,3′,5,5′-tetramethylbenzidine (TMB) was used as the substrate for the enzyme reaction while the blank sample comprised a 10 mM PBS solution containing Alexa Fluor™ 488 at 50 μM to allow confirmation of the fluid flow. The reagent flows through the micro-/nanochannels were adjusted using a pressure controller (MFCS-EZ, Fluigent, Paris, France; ARGOS, Institution of Microchemical Technology, Kanagawa, Japan), and the flows were observed with a fluorescence microscope (IX73, Olympus Corp., Tokyo, Japan). The detector was a DIC-TLM system using two lasers producing a 20 mW excitation beam at 660 nm and a 1.5 mW probe beam at 532 nm.

4. Results and Discussion

4.1. Operation of multiple valves

In order to align the multiple actuators with the multiple valves in this device, the center positions of the jig holes were determined, as summarized in Table S1. In addition, the results of operating multiple valves are provided in Fig. 5. Figure 5(a) shows the positional errors for the actuators and valves following the initial placement of the unit in its holder. An alignment stage capable of fixing the lower jig with the device and holding the upper jig containing the actuators while controlling the XY position as well as the angle, θ, in the XY plane was developed. The alignment procedure was carried out under observation with a microscope to confirm a suitable degree of control over the position of the actuators and achieve positioning errors of less than 20 μm (the developed alignment stage is shown in Supplementary Information, Fig. S3). Figure 5(b) presents images of the valves and the actuators. Although the distances between the actuators and the valves were initially on the order of 100 μm or more, the positions were eventually aligned as a result of using the specially designed stage.

Then, the actuators were extended by applying a voltage of 100 V, and the vertical position of the actuators were lowered by tightening the screw on the top until it closed the valve. The voltage supply to the actuator was then turned off and the valve was opened. Because the displacement of the piezoelectric actuators is about 5 μm, which is much larger than the valve depth (100 nm), the valve operation can be achieved, and the accuracy of aligning the vertical position is < 5 μm.

After alignment was accomplished, two valves (A and B) located with a distance of 3.5 mm were used to demonstrate multi-valve operation (Fig. 5(c)). The microchannels, nanochannels and valve chambers were initially filled with a 100 μM solution of Alexa Fluor™ 488 in PBS. Subsequently, the valve was opened/closed by turning the voltage off and on, respectively. After closing valve B, valve A was repeatedly opened and closed and the open/close state of each valve was observed using a fluorescence microscope (IX73, Olympus Corp., Tokyo, Japan). As shown in Fig. 5(d), valve B remained closed during the operation of valve A. Although only two valves were used in this experiment, the results suggest that

deformation of the entire device caused by valve operation was reduced to a sufficiently small value, in agreement with the results of the simulations. These tests confirmed the functioning of the reinforcement installed in the lower jig and showed that the alignment of multiple valves successfully resulted in independent operation of these valves.

Figure 6(a) shows the fabricated device for verifying repeated fluid operation using multiple valves. Two nanochannels are connected to one nanochannel, each with a valve at the connection point. The width and depth of the nanochannels were 5 μm and 2 μm respectively. The nanochannels are connected to microchannels for flow injection. The fluid operation is described in Fig. (b). In the initial state, PBS and 100 μM fluorescein solution prepared with PBS were filled in the microchannels at the upstream of valves 1 and 2 respectively, applying a pressure of 100 kPa. The nanochannels were filled with PBS as well. When valve 1 was closed and valve 2 was opened for 1 s, a certain volume of fluorescein was flowed in the nanochannel. As valve 2 was closed and valve 1 was opened simultaneously, the flow switched to the flow of PBS, which transported the injected fluorescein to the downstream. The fluid operation was confirmed from fluorescence observation (Fig. (c)). Figure (d) shows the fluorescence intensity measured at a point 600 μm downstream of valve 2. The operation was successfully repeated for more than 50 times. We have confirmed that the valve can endure more than 100,000 times of open/close operation in our previous work.[28] Therefore, repeated fluid operations using multiple valve could also be achieved. In addition, the relative standard deviation of the peak area was 1.6 %, which is lower than our conventional injection method using pressure (~ 5 %).[34] This result indicates that reproducible and more promising fluid operation can be achieved by valve control.

4.2. Demonstration of ELISA

The device used for the ELISA demonstration is shown in Fig. 7. This unit contained microchannels with widths of 400 μm and depths of 20 μm, along with nanochannels having a width and depth of 3 and

1.2 μm, respectively. A total of seven valves (V1 to V7) were fabricated between the nanochannels to control the flow, each with a diameter of 75 μm and a depth of 100 nm. The depth direction for each comprised four 25 nm-deep steps. In addition to the valves, a pipette with a volume of 25 pL and an ELISA channel with a 3 mm-long antibody capture region were successfully fabricated.

Figure 8 provides representative results from an ELISA trial performed based on the unit operations listed in Fig. 4. The sample solution and washing buffer was initially introduced at 40 kPa and 50 kPa respectively while all valves except V2 and V3 were closed. These pressures were employed so that the sample solution and the washing buffer does not mix in the nanochannel and dilute the sample. The sample flowed through V2 and V3 and filled the pipette placed in between (Fig. 8(a)). Because V1 and V4 were closed at this point, the flow in both directions was blocked and the sample flowed out to the drain. Following this, V2 and V3 were closed and the volume of 25 pL between the two valves was isolated (Fig. 7(b)). Washing buffer was then introduced from the upstream of V1 at 120 kPa. Upon opening V1 and V4, the washing buffer pushed this sample downstream to the ELISA channel where the antigen (Ag)-antibody (Ab) reaction occurred (Fig. 8(b)(c)). After the time required for transportation to the ELISA channel (which was determined beforehand) had elapsed, V4 was closed so that the sampling region and ELISA region were partitioned. To allow bound/free (B/F) separation, washing buffer was introduced by opening V5, and V6 was then opened so that the HRP-conjugated antibody solution flowed into the ELISA channel. V5 was opened again for B/F separation and V7 was opened to introduce the TMB into the ELISA channel to promote the enzymatic reaction. One minute after opening V7, the flow was stopped by closing V7 to allow formation of colored substrates. After 90 s, V7 was opened again to transport the colored substrates to the detection point. In this manner, all the chemical processes and flow operations required for the ELISA technique were conducted based on the opening and closing of multiple valves. Figure 9 provides the signal obtained from DIC-TLM. The signal obtained from IL-6 molecules captured in the ELISA channel was determined by the flow rate and the distance between the detection point and

the area where the capture antibody was immobilized. The signal from IL-6 molecules is within the purple region shown in Fig.9. The peaks outside the region and the small peak in the blank solution are considered as signals due to non-specific adsorption of HRP-conjugated antibodies. The injected sample consisted of 25 pL of a 100 pM solution and so the signal obtained from the captured IL-6 resulted from at most 1,500 molecules (considering sample loss due to non-specific adsorption). Based on prior work by our group, this number can be considered to equal the quantity of IL-6 molecules secreted by a single Raji B cell in 7.3 hours in response to a mixture of 12-myristate 13-acetate and ionomycin, which is similar to the condition in our previous study.[35] Therefore, the performance of the system developed in this study is sufficient to allow single-cell analysis. In conclusion, a signal was obtained from a small number of molecules based on the ELISA process, confirming the operation of the present nanofluidic analytical system with integrated valves. Conventionally, micro-/nanofluidic analyses are performed by controlling the fluid using a driving pressure because integration of practical valves into glass-based nanofluidic devices has not been feasible to date. For this reason, it has been difficult to perform nanofluidic unit operations and even more challenging to integrate these operations to create a complete analytical system. Thus, to date, such systems have been unstable and require a high degree of skill and significant experience to operate. Because the valves in the device described herein function on a simple open/close basis and a robust method is used to control the fluid flows, this novel analytical system suggests a wider range of possible applications for nanofluidic devices in various fields, such as single-cell proteomics.

5. Conclusions

This study developed a nanofluidic analytical system integrated with nanochannel open/close valves and verified the operation of this new system. This device comprised pneumatic pumps for fluid injection, piezo actuators used to control fluid flows based on valve operations, and a detector. When operating multiple valves, micrometer-scale deformation of the entire device resulting from the application of a

mechanical force on the order of 1 N to the valves was found to affect other valves and make individual valve operation impossible. Consequently, a reinforcement for the device holder was designed to restrict such deformations to the nanometer scale and to enable independent operation of the valves. This research also revealed that the actuators and the valves had to be aligned within an error of less than 20 μm in order to allow proper opening and closing of the valves. An alignment system was devised to set the positions of the actuators with the required precision. Finally, IL-6 molecules were analyzed by ELISA as a demonstration of the operation of the newly developed system. Fluid operations during this analysis, such as flow switching and sampling, were successfully achieved by operating multiple valves, and a DIC-TLM signal from approximately 1,500 IL-6 molecules was obtained. This work represents the first-ever demonstration of nanofluidic analysis predicated on controlling fluid flows using multiple nanochannel open/close valves. The simple and robust control of fluid based on the operation of multiple valves as demonstrated herein is expected to become an essential aspect of realizing the use of integrated micro-/nanofluidic devices in various fields.

Conflicts of Interest

There are no conflicts of interest to declare.

Acknowledgement

The authors gratefully acknowledge financial support from the Core Research for Evolutional Science and Technology (CREST) program of the Japan Science and Technology Agency (JST) via grant no. JPMJCR14G1. This work was also supported in part by the Ministry of Science and Technology, Taiwan, via grant nos. MOST 109-2639-E-007-001-ASP and MOST 110-2639-E-007-002-ASP.

References

1 C. Y. Lee, C. L. Chang, Y. N. Wang and L. M. Fu, *Int. J. Mol. Sci.*, 2011, **12**, 3263–3287.

2 G. H. Seong and R. M. Crooks, *J. Am. Chem. Soc.*, 2002, **124**, 13360–13361.

3 D. Ciceri, J. M. Perera and G. W. Stevens, *J. Chem. Technol. Biotechnol.*, 2014, 89, 771–786.

4 M. Sivaramakrishnan, R. Kothandan, D. K. Govindarajan, Y. Meganathan and K. Kandaswamy, *Curr. Opin. Biomed. Eng.*, 2020, **13**, 60–68.

5 P. S. Dittrich, K. Tachikawa and A. Manz, *Anal. Chem.*, 2006, **78**, 3887–3908.

6 W. Lee, W. Fon, B. W. Axelrod and M. L. Roukes, *Proc. Natl. Acad. Sci. U. S. A.*, 2009, **106**, 15225–15230.

7 J. Jiang, H. Zhao, W. Shu, J. Tian, Y. Huang, Y. Song, R. Wang, E. Li, D. Slamon, D. Hou, X. Du, L. Zhang, Y. Chen and Q. Wang, *Sci. Rep.*, 2017, **7**, 1–11.

8 W. H. Grover, A. M. Skelley, C. N. Liu, E. T. Lagally and R. A. Mathies, *Sensors Actuators, B Chem.*, 2003, **89**, 315–323.

9 W. Zhang, S. Lin, C. Wang, J. Hu, C. Li, Z. Zhuang, Y. Zhou, R. A. Mathies and C. J. Yang, *Lab Chip*, 2009, **9**, 3088–3094.

10 H. K. Ma, B. R. Hou, C. Y. Lin and J. J. Gao, *Int. Commun. Heat Mass Transf.*, 2008, **35**, 957–966.

11 D. J. Beebe, J. S. Moore, J. M. Bauer, Q. Yu, R. H. Liu, C. Devadoss and B.-H. Jo, *Nature*, 2000, **404**, 588–590.

12 R. Pal, M. Yang, B. N. Johnson, D. T. Burke and M. A. Burns, *Anal. Chem.*, 2004, **76**, 3740–3748.

13 D. Accoto, M. C. Carrozza and P. Dario, *J. Micromechanics Microengineering*, 2000, **10**, 277–281.

14 C. Yamahata, F. Lacharme, Y. Burri and M. A. M. Gijs, *Sensors Actuators, B Chem.*, 2005, **110**, 1–7.

15 D. Mark, T. Metz, S. Haeberle, S. Lutz, J. Ducrée, R. Zengerle and F. von Stetten, *Lab Chip*, 2009, **9**, 3599–3603.

16 H. Cho, H. Y. Kim, J. Y. Kang and T. S. Kim, *J. Colloid Interface Sci.*, 2007, **306**, 379–385.

17 M. A. Unger, H.-P. Chou, T. Thorsen, A. Scherer and S. R. Quake, *Science*, 2000, **288**, 113–116.

18 T. Thorsen, S. J. Maerkl and S. R. Quake, *Science*, 2002, **298**, 580–584.

19 I. E. Araci and S. R. Quake, *Lab Chip*, 2012, **12**, 2803–2806.

20 S. L. Spurgeon, R. C. Jones and R. Ramakrishnan, *PLoS One*, 2008, **3**, 1–7.

21 Y. Xin, J. Kim, M. Ni, Y. Wei, H. Okamoto, J. Lee, C. Adler, K. Cavino, A. J. Murphy, G. D. Yancopoulos, H. C. Lin and J. Gromada, *Proc. Natl. Acad. Sci. U. S. A.*, 2016, **113**, 3293–3298.

22 K. Mawatari, Y. Kazoe, H. Shimizu, Y. Pihosh and T. Kitamori, *Anal. Chem.*, 2014, **86**, 4068–4077.

23 K. Shirai, K. Mawatari, R. Ohta, H. Shimizu and T. Kitamori, *Analyst*, 2018, **143**, 943–948.

24 K. Yamamoto, K. Morikawa, H. Imanaka, K. Imamura and T. Kitamori, *Analyst*, 2020, **145**, 5801–5807.

25 R. Ishibashi, K. Mawatari and T. Kitamori, *J. Chromatogr. A*, 2012, **1238**, 152–155.

26 T. Nakao, Y. Kazoe, E. Mori, K. Morikawa, T. Fukasawa, A. Yoshizaki and T. Kitamori, *Analyst*, 2019, **144**, 7200–7208.

27 Y. Kazoe, Y. Pihosh, H. Takahashi, T. Ohyama, H. Sano, K. Morikawa, K. Mawatari and T. Kitamori, *Lab Chip*, 2019, **19**, 1686–1694.

28 H. Sano, Y. Kazoe, K. Morikawa and T. Kitamori, *Microfluid. Nanofluidics*, 2020, **24**, 1–11.

29 H. Shimizu, K. Mawatari and T. Kitamori, *Anal. Chem.*, 2010, **82**, 7479–7484.

30 COMSOL Multiphysics® v. 5.6., www.comsol.com, COMSOL AB, Stockholm, Sweden.

31 M. Tokeshi, T. Minagawa, K. Uchiyama, A. Hibara, K. Sato, H. Hisamoto and T. Kitamori, *Anal. Chem.*, 2002, **74**, 1565–1571.

32 K. Morikawa, Y. Kazoe, Y. Takagi, Y. Tsuyama, Y. Pihosh, T. Tsukahara and T. Kitamori, *Micromachines*, 2020, **11**, 1–11.

33 K. Shirai, K. Mawatari and T. Kitamori, *Small*, 2014, **10**, 1514–1522.

34 M. Kato, M. Inaba, T. Tsukahara, K. Mawatari, A. Hibara and T. Kitamori, *Anal. Chem.*, 2010, **82**, 543–547.

35 T. Nakao, Y. Kazoe, E. Mori, K. Morikawa, T. Fukasawa, A. Yoshizaki and T. Kitamori, *Analyst*, 2019, **144**, 7200–7208.

Figures

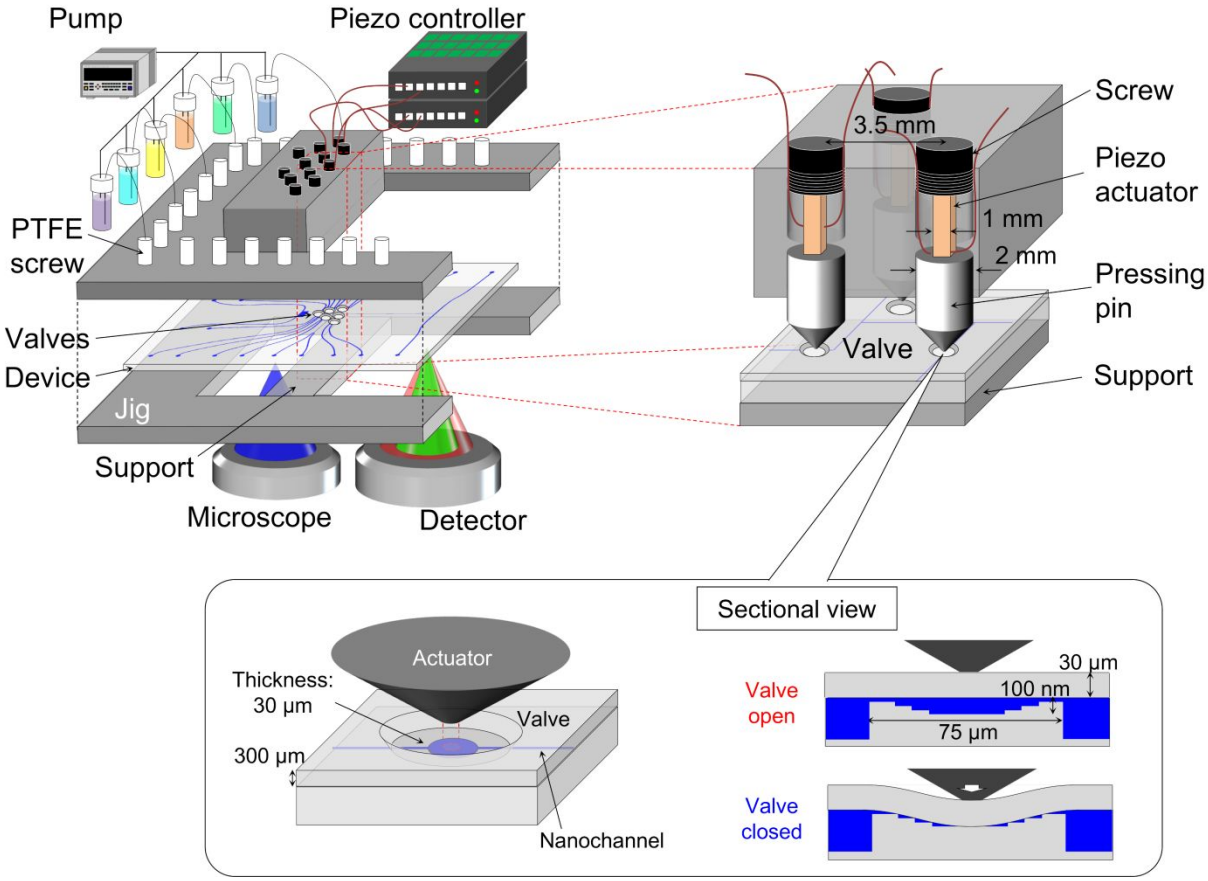

Figure 1. The design of the integrated analytical system comprising pumps, piezo controllers and a detector. The jig contained orifices to allow the setting of piezoelectric actuators and valve pressing pins. Each valve consisted of a deformable part fabricated over a small area and a four-step valve chamber. Each deformable part had a thickness of 30 µm to permit glass deformation as a means of opening/closing the nanochannel.

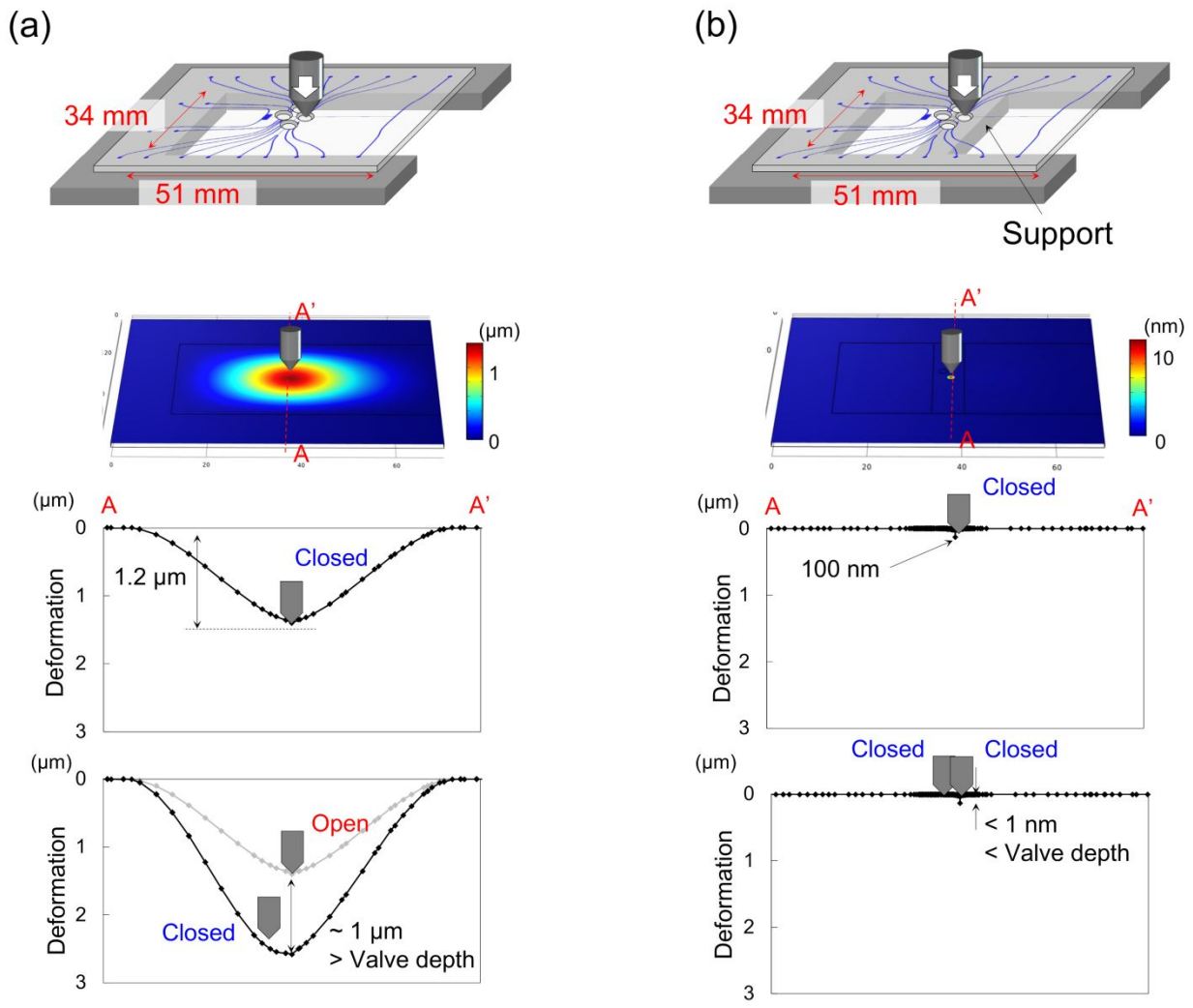

Figure 2. Results from calculations of device deformation. (a) Without support under the valves, such that pressing the second valve will deform the entire device and cause the first valve to open. (b) With support under the valves, such that device deformation caused by pressing the second valve will not affect the closed state of the first valve.

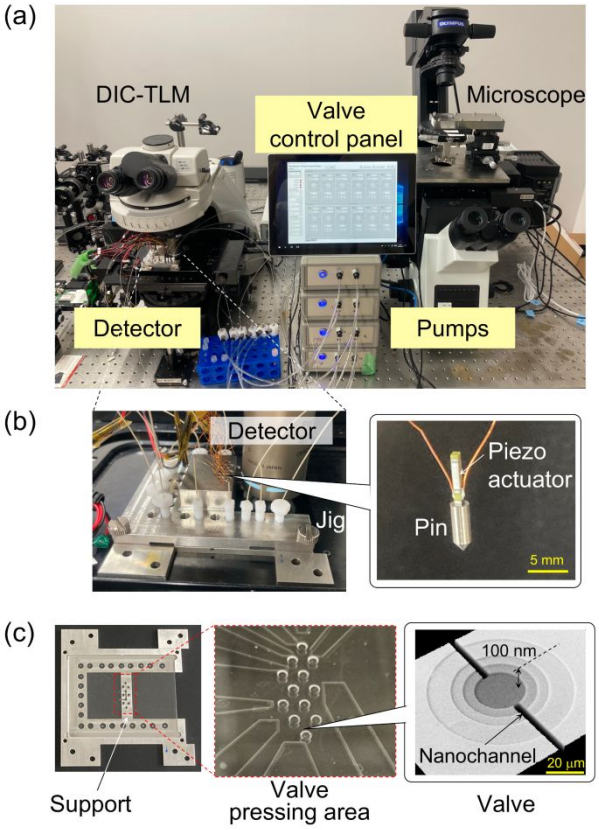

Figure 3. The system developed in the present work. (a) The flow inside the device is observed using a fluorescence microscope while the jig is moved to the stage of the DIC-TLM for detection. (b) Piezo actuators are inserted into pressing pins and set inside the jig. (c) A support was fabricated and inserted under the valve area and the four-step valve chamber.

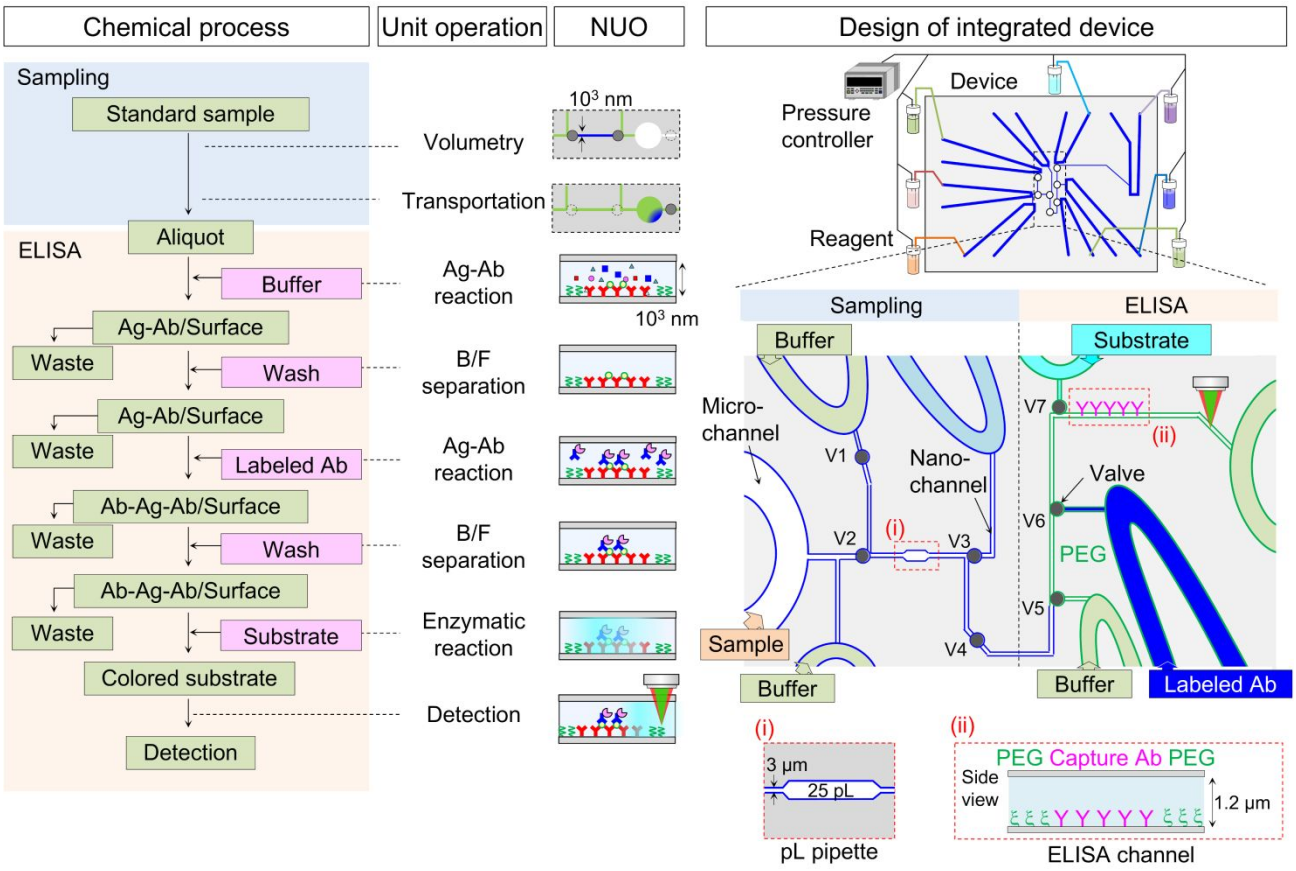

Figure 4. Flow chart of the ELISA process and a conversion to unit operations and NUOs. A total of seven valves was designed to integrate all NUOs into the device.

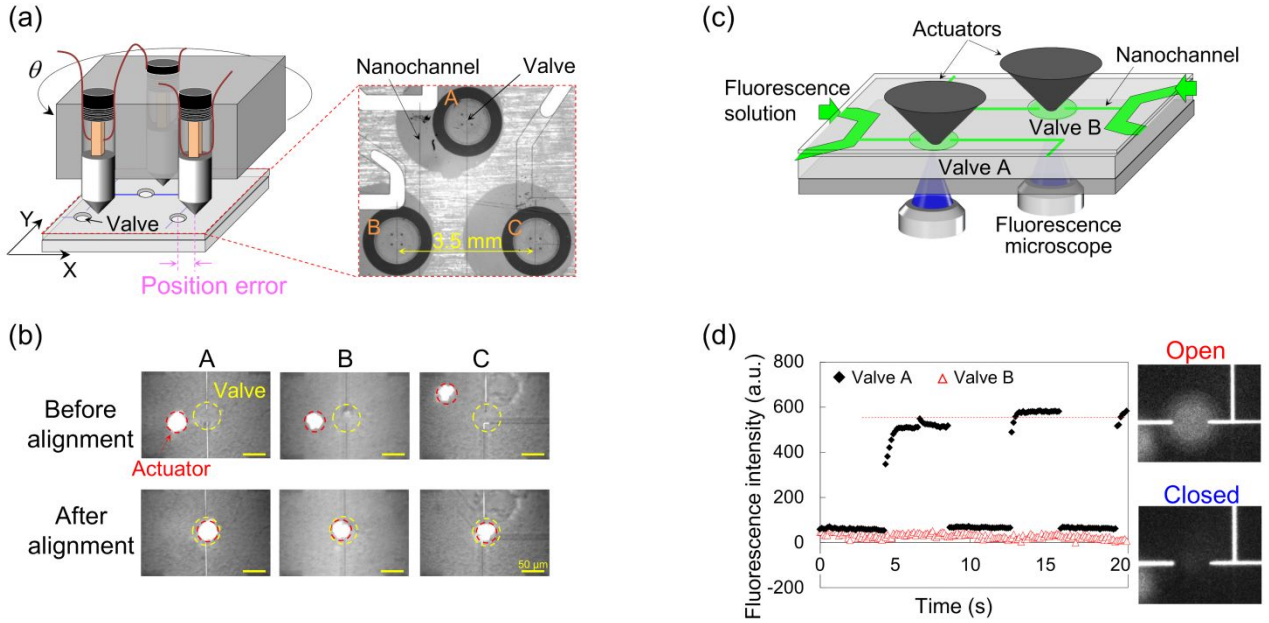

Figure 5. (a) Schematic of the alignment of the valves and the actuators. (b) Images of the valves and the actuators before and after alignment using the alignment system. (c) Experimental setup for verifying the independent operation of multiple valves. (d) Fluorescence intensity values obtained from the two valve chambers (A and B).

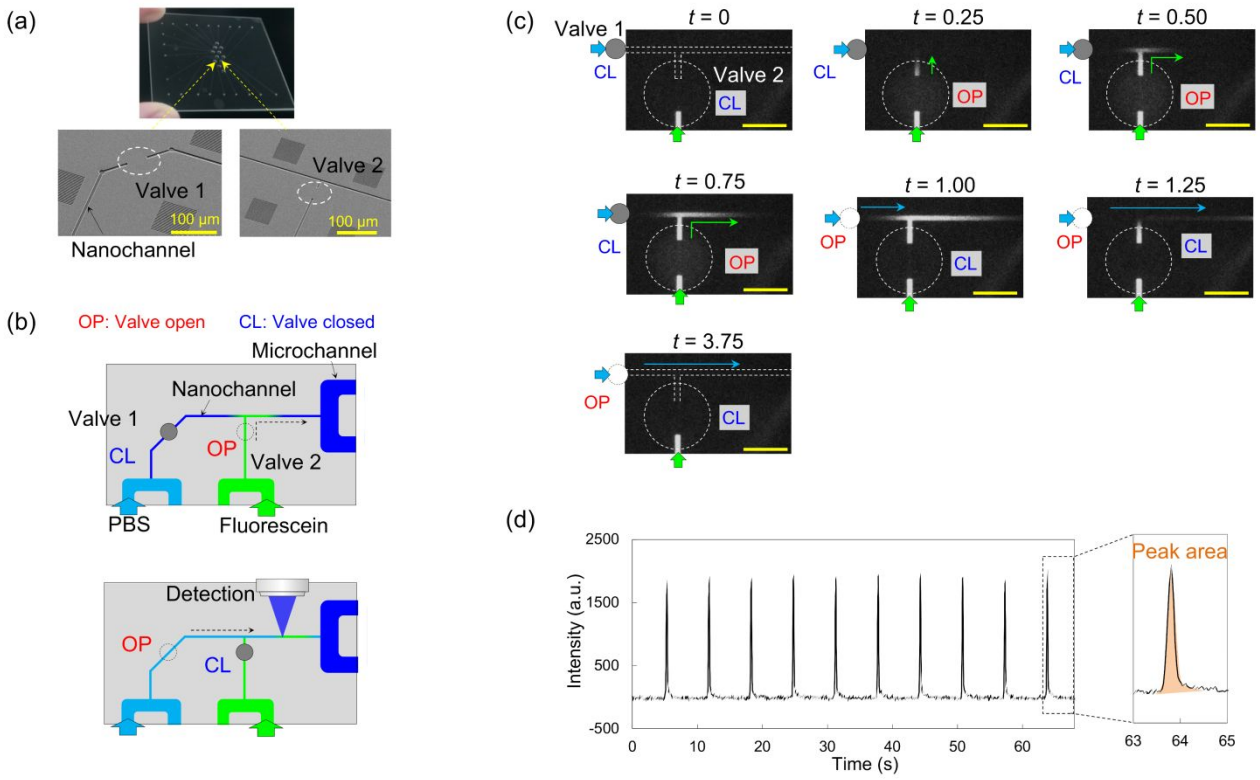

Figure 6. Experimental results of fluid operation using multiple valves. (a) Photograph and scanning electron microscope (SEM) image of fabricated device, (b) operation of valves, (c) fluorescence image during the fluid operation, and (d) fluorescence intensity measured at a point 600 μm downstream of valve 2.

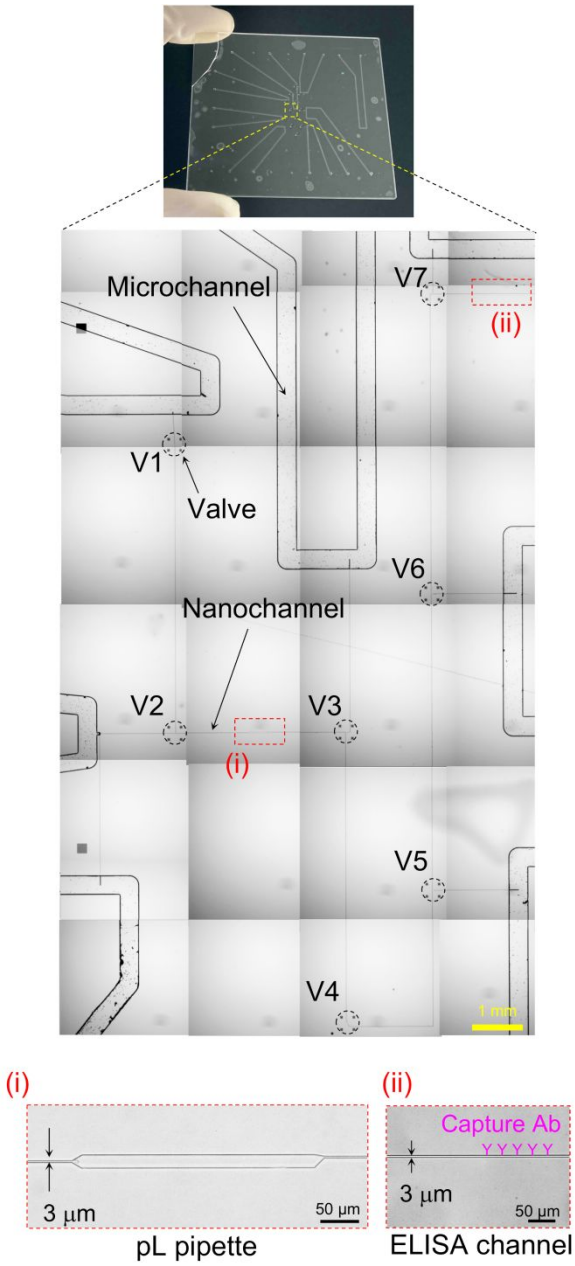

Figure 7. Image of the fabricated device, in which microchannels, nanochannels and seven valves were successfully fabricated.

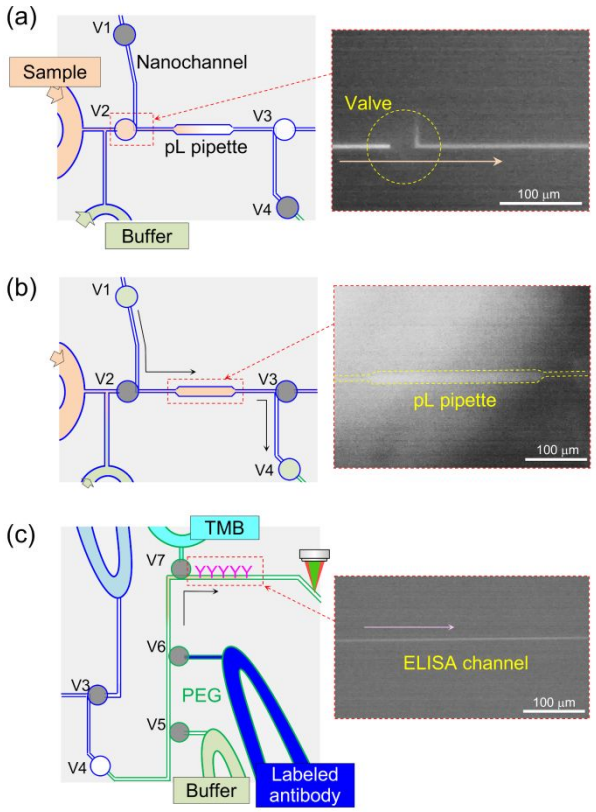

Figure 8. Fluid operations using the valves. (a) Sample injection: V2, V3 opened / V1, V4-7 closed. (b) Sample transportation: V1, V4 opened / V2,V3, V5-7 closed. (c) V1, V4 opened / V2,V3, V5-7 closed. The transportation of the sample solution to the ELISA channel was confirmed.

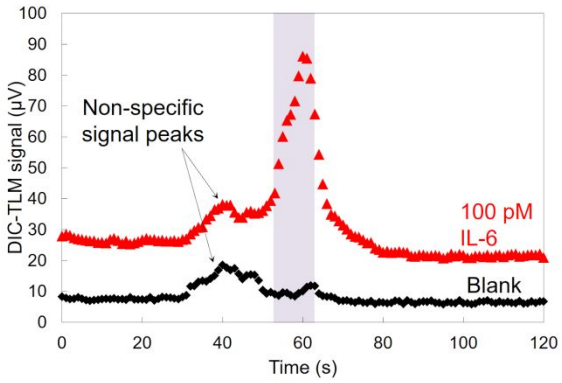

Figure 9. Signal obtained from the DIC-TLM. The purple region indicates the time range of the signal obtained from the area in which the capture antibody was immobilized.